

Primary and secondary order parameters in the fully frustrated transverse-field Ising model on the square lattice

Gabe Schumm^{1,*}, Hui Shao,^{2,3} Wenan Guo^{4,3}, Frédéric Mila^{5,†} and Anders W. Sandvik^{1,6,‡}

¹*Department of Physics, Boston University, 590 Commonwealth Avenue, Boston, Massachusetts 02215, USA*


²*Center for Advanced Quantum Studies, Department of Physics, Beijing Normal University, Beijing 100875, China*

³*Key Laboratory of Multiscale Spin Physics, Ministry of Education, Beijing 100875, China*

⁴*Department of Physics, Beijing Normal University, Beijing 100875, China*

⁵*Institute of Physics, Ecole Polytechnique Fédérale de Lausanne (EPFL), CH-1015 Lausanne, Switzerland*

⁶*Beijing National Laboratory for Condensed Matter Physics and Institute of Physics, Chinese Academy of Sciences, Beijing, 100190, China*

 (Received 7 September 2023; revised 4 January 2024; accepted 11 April 2024; published 26 April 2024)

Using quantum Monte Carlo simulations and field-theory arguments, we study the fully frustrated transverse-field Ising model on the square lattice for the purpose of quantitatively relating two different order parameters to each other. We consider a “primary” spin order parameter and a “secondary” dimer order parameter, which both lead to the same phase diagram but detect \mathbb{Z}_8 and \mathbb{Z}_4 symmetry breaking, respectively. While at $T > 0$ their scaling exponents are simply related to each other, as explained by a mapping to a height model, we show that at $T = 0$ they correspond to different charge sectors of the $O(2)$ model in $2 + 1$ dimensions with nontrivial exponents that are not simply related to each other. Our insights are transferrable to a broad class of Ising models whose low-energy physics involves dimer degrees of freedom, and also serve as a guide to treating primary and secondary order parameters more generally.

DOI: [10.1103/PhysRevB.109.L140408](https://doi.org/10.1103/PhysRevB.109.L140408)

Introduction. The concept of an order parameter is key to quantitative descriptions of phase transitions. In some systems it is natural to define more than one order parameter, either in some trivial way or using emergent degrees of freedom originating from some mapping to an effective low-energy model. The relationships between different order parameters may be nontrivial, e.g., unexplained behavior of a “parasitic” ferromagnetic order parameter in a system with primarily antiferromagnetic order was reported [1–3]. Here we consider a quantum spin model that very clearly illustrates two different order parameters that not only exhibit different scaling behaviors but the relationships between the critical exponents of the order parameters are also different at temperature $T = 0$ and $T > 0$.

We study the two-dimensional (2D) square-lattice fully frustrated transverse field (Villain) quantum Ising model (FFTFIM), with Hamiltonian

$$H = \sum_{\langle ij \rangle} J_{ij} \sigma_i^z \sigma_j^z - \Gamma \sum_j \sigma_j^x, \quad (1)$$

where σ_i^x and σ_i^z are Pauli operators. The couplings J_{ij} are equal in magnitude but the number of antiferromagnetic (AF) couplings around any elementary plaquette is odd [4], here with $J_{ij} = +J$ (AF) on every second column and $J_{ij} = -J$

on all other bonds as depicted in Fig. 1. The classical model at $\Gamma = 0$ hosts a large ground state degeneracy that is lifted by the transverse field via an “order-by-disorder” mechanism [5–7].

The first studies of the FFTFIM considered the stacked version of the classical model using a Landau-Ginsburg-Wilson (LGW) approach [8] as well as Monte Carlo (MC) simulations [9]. The LGW study predicted an eight-fold degenerate ground state, which was more precisely characterized by Ref. [9] as a \mathbb{Z}_4 symmetry breaking phase, corresponding to 90° rotations of the lattice, paired with a global spin-flip symmetry.

The model was later treated using quantum MC (QMC) simulations [10], where spin and dimer order was found at $T = 0$ for $\Gamma < \Gamma_c \sim 1.578$. In this phase the frustrated bonds (mapped to dimers as in Fig. 1) align along alternating columns or rows; the \mathbb{Z}_4 symmetry breaking phase identified in the stacked model. The order parameters considered previously detected \mathbb{Z}_4 symmetry and spin-reflection symmetry separately. The reconciliation of \mathbb{Z}_8 versus \mathbb{Z}_4 breaking was touched on by Coletta *et al.* [11], but the relationship between the respective order parameters was not explored.

Here we define a proper \mathbb{Z}_8 symmetric spin order parameter and demonstrate that the \mathbb{Z}_4 dimer order parameter should be considered as *secondary*. While both order parameters lead to the same phase diagram (provided in Supplemental Material, Sec. SI [12]), the \mathbb{Z}_4 order parameter exhibits faster decaying critical correlations. Both order parameters, when correctly defined, exhibit emergent $U(1)$ symmetry in the critical phase as well as at the quantum phase transition, stemming

*gschumm@bu.edu

†frederic.mila@epfl.ch

‡sandvik@bu.edu

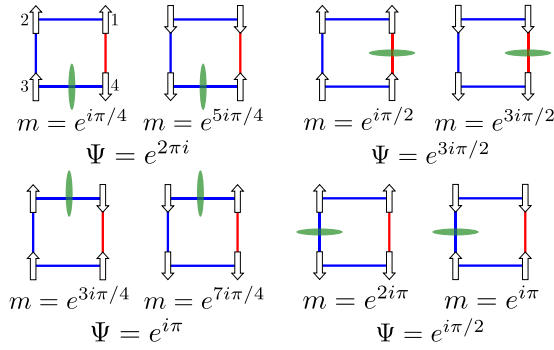


FIG. 1. The degenerate ground states represented by elementary plaquettes. Blue and red bonds show $J_{ij} = -J$ and $J_{ij} = +J$, respectively. The direction of the sublattice magnetizations m_s , $s = 1, \dots, 4$, are indicated by the arrows, and dimers (green ovals) are defined on the frustrated bonds. The values of the magnetization and dimer order parameters shown correspond to the ground state sublattice magnetizations of the stacked, classical ($\Gamma = 0$) model [8], $\sin(\pi/8)$ for the sites sharing a frustrated bond and $\cos(\pi/8)$ for the two others [see Eqs. (3) and (5)].

from the irrelevance of the discrete symmetry-breaking terms at criticality [13]. However, the distinction between primary and secondary order is made quantitative by considering the critical scaling in these two regimes. This is only made possible by connecting these order parameters to operators in the relevant field theories, at $T = 0$ and $T > 0$. Finite-size scaling of QMC (stochastic series expansion [14]) results of the full FTFIM Hamiltonian, Eq. (1), support the predicted scaling, emphasizing the utility of this novel approach to studying quantum magnetism.

Secondary order parameters have previously been used to describe higher harmonic contributions to spatial modulation in density wave systems, e.g., liquid crystals [15–19]. A secondary order parameter can clearly be defined also in the FTFIM, but the different scaling forms of the spin and dimer order parameter in the FTFIM have not been addressed. This Letter provides a framework for secondary order not just in the FTFIM, but in the entire class of frustrated Ising models with effective dimer degrees of freedom, e.g., the antiferromagnet on the triangular lattice [20–24].

Order Parameters. To construct a proper primary order parameter, we follow standard procedures [8,11,22], using an effective Hamiltonian for the amplitude m and phase θ of critical modes:

$$H_{\text{eff}} = \sum_{\vec{q}} (r + q^2)|m|^2 + u_4|m|^4 + u_6|m|^6 + (u_8 + v_8/32)|m|^8 - (v_8/32)|m|^8 \cos(8\theta). \quad (2)$$

The eight-state clock anisotropy implies an eight-fold degenerate ground state, characterized by sublattice magnetizations (m_1, m_2, m_3, m_4) ; see Fig. 1. Each state corresponds to one frustrated bond in a plaquette, where the magnitude of the sublattice magnetizations of the sites sharing this bond are smaller than the other two, $\sin(\pi/8)$ and $\cos(\pi/8)$, respectively [8]. An overall spin-flip transformation gives a total of eight degenerate states.

Based on the low-energy behavior of the stacked model, as well as the semiclassical analysis of Ref. [11], we define the primary order parameter as the complex number

$$m = m_x + im_y = \frac{1}{2}(m_1 e^{i\pi/8} + m_2 e^{i3\pi/8} + m_3 e^{i5\pi/8} + m_4 e^{i7\pi/8}), \quad (3)$$

where

$$m_s = \frac{4}{N} \sum_{j \in s} \sigma_j^z. \quad (4)$$

The eight ground state configurations of the stacked model correspond to $m = e^{in\pi/4}$, $n = 1, 2, \dots, 8$.

The problem can also be mapped onto that of dimer coverings, where a dimer is assigned across each frustrated bond [23], and we define a secondary order parameter Ψ with this mapping in mind. This order parameter is also complex number, defined in terms of the dimer density modulation on the dual lattice [10]:

$$\Psi = \Psi_x + i\Psi_y = 2\tilde{d}_x(0, \pi) + 2i\tilde{d}_y(\pi, 0), \quad (5)$$

where

$$\tilde{d}_\alpha(\mathbf{q}) = \frac{1}{N} \sum_i e^{i\mathbf{q} \cdot \mathbf{r}_i} d_{i,\alpha}, \quad (6)$$

is the Fourier transformed dimer density

$$d_{i,\alpha} = 1 + \frac{J_{i,j_\alpha}}{J} \sigma_i^z \sigma_{j_\alpha}^z, \quad (7)$$

and j_α is the index of nearest neighbor to site i in the α direction. Long-range ordering is associated with $|\Psi|$ taking a finite value, while the specific (symmetry-broken) ordering pattern is identified by the phase. Thus, Ψ takes one out of the values $e^{in\pi/2}$, $n = 1, 2, \dots, 4$. The connection between the columnar states and the sublattice magnetizations is illustrated in Fig. 1.

\mathbb{Z}_8 versus \mathbb{Z}_4 Symmetry Breaking. We detect the order-parameter symmetries by plotting the probability distributions of m and Ψ accumulated during QMC simulations. In the ordered phase, we expect eight (four) δ functions at the eight (four) values corresponding to the columnar spin (dimer) states in Fig. 1. These δ -functions smear for finite systems, appearing as highly peaked Gaussian distributions for large systems.

In the critical phase, we observe the emergent U(1) symmetry expected from the mapping to the height model [25–27]. We assign height differences to neighboring spins based whether or not the bond they share is frustrated (i.e., crossing a dimer) [26], as detailed in the Supplemental Material, Sec. SII [12]. In the ordered phase, the height profile is “flat,” with the height values bounded from above. In the critical and disordered phases, the model is in its “rough” phase, with a logarithmically diverging height profile. This behavior can be described by an effective elastic free energy with a periodic “locking” potential favoring the eight flat height configurations, i.e., the columnar states in Fig. 1. This effective free energy is precisely that of the 2D XY model, where the locking potential corresponds to an $q = 8$ state clock anisotropy term. This connection allows us to apply the

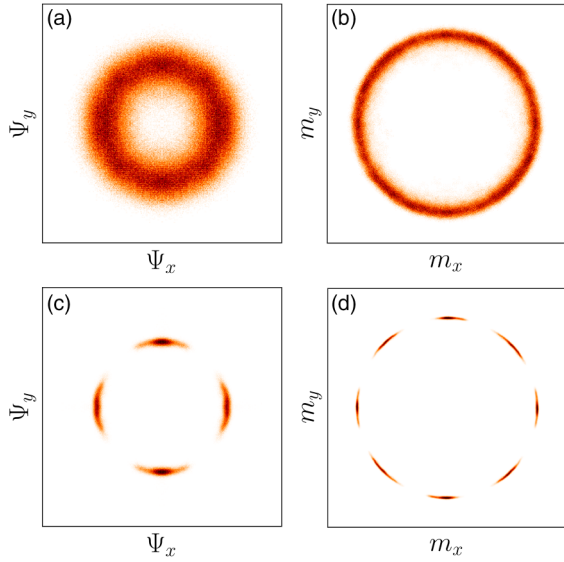


FIG. 2. Distributions of (Ψ_x, Ψ_y) in (a), (c) and (m_x, m_y) in (b), (d), collected in several independent simulations (each initialized in one of the four columnar states, to prevent trapping in states with topological defects) and symmetrized using lattice rotations and reflections. The system size is $L = 96$ and $\Gamma/J = 0.43$, with $T/J = 0.21$ in (a), (b) (in the critical phase) and $T/J = 0.014$ in (c), (d) (in the ordered phase).

renormalization group analysis of Ref. [13] to understand the observed behavior.

Jose *et al.* [13] first showed that the classical 2D q -state clock model is characterized by three temperature regimes if $q > 4$. At temperatures below the lower critical temperature T_{c1} , the clock term is relevant and the system orders into the \mathbb{Z}_q clock phase. At T above T_{c1} but below the upper critical temperature T_{c2} , the clock term is irrelevant and the free energy reduces to that of the XY model in the Kosterlitz–Thouless (KT) phase. In this phase, the system can freely fluctuate between the flat height configurations, thus resulting in the U(1) symmetric distributions that we observe. Finally, above T_{c2} the critical phase melts into the disordered phase as defects proliferate.

An example of the symmetry reduction in the ordered phase is shown in Fig. 2, where (a) and (b) are collected from simulations in the critical phase, while (c) and (d) are from the ordered phase. While we detect emergent U(1) symmetry in both order parameters, a U(1) phase would not be expected for a primary \mathbb{Z}_4 dimer order parameter at $T > 0$, given the $q > 4$ criterion in the clock model [13]. However, with the spin order parameter corresponding to $q = 8$, the critical phase is expected.

Scaling at $T > 0$. As a quantitative characterization of the primary and secondary natures of the two order parameters, we compare the scaling of their respective correlation functions in the critical phase. Within the q -state clock-model description, the spin-spin correlations should decay algebraically with a scaling exponent η that varies continuously with the temperature [28]. The value of η at the upper and lower critical temperatures are known, $\eta = 1/4$ and $\eta = 4/q^2$, respectively [13,27]. To extract η , we examine the magnitudes

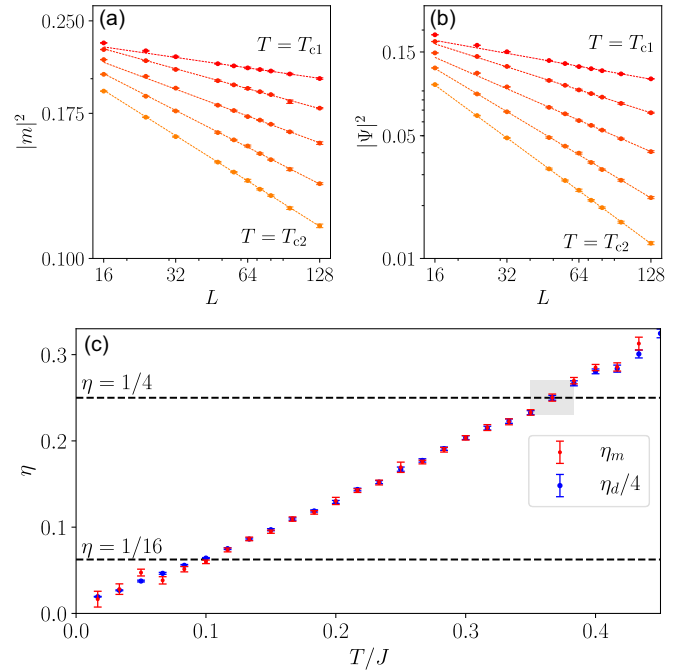


FIG. 3. Log-log plots of the magnitude of the primary (a) and secondary (b) order parameter versus the system size L for a range of temperatures at $\Gamma/J = 0.67$. The dashed lines are power-law fits to the largest eight system sizes, with T increasing with color brightness (red to orange). (c) Anomalous dimensions $\eta_{m,d}$ versus T for the primary (red) and secondary (blue) order parameters, extracted from fitting data to Eq. (8). The exponents align if η_d is rescaled by a factor $1/4$. The gray box denotes $T_{c2} \pm \sigma$ from Binder crossing results. The dashed lines are at the predicted values at the phase boundaries.

of both order parameters, which in this phase should scale with the lattice length L as

$$|m|^2 \propto L^{-\eta_m}, \quad |\Psi|^2 \propto L^{-\eta_d}, \quad (8)$$

where we leave open the possibility that $\eta_m \neq \eta_d$. In Fig. 3(a) and 3(b), the order parameters are plotted versus system size for a range of temperatures between T_{c1} and T_{c2} . As predicted, they scale algebraically with L , and we extract $\eta_m(T)$ and $\eta_d(T)$ by fitting data to Eq. (8). The results are shown versus T in Fig. 3(c).

The primary order parameter scales with the expected exponent $\eta_m = 1/4$ at the upper critical temperature T_{c2} extracted from Binder crossing results (Supplemental Information, Sec. SI [12]). Below this temperature, the exponent linearly decreases. The statistical quality of the fits deteriorates below the temperature at which $\eta_m = 1/16$ (see Supplemental Material, Sec. SIII [12]), which is the predicted value at the lower transition point T_{c1} [13], where the system orders. While the linear decrease in η appears to continue below T_{c1} , the deterioration of the power-law fit used to extract the exponents below this temperature implies that this trend should not be given any credence. Thus, our numerical results are consistent with the theory, and we can use $\eta_m = 1/4$ and $\eta_m = 1/16$ to set more precise upper and lower boundaries.

The same behavior is observed for the dimer order parameter, except that the value of the η_d is consistently approximately four times larger than η_m . After rescaling η_d

by a factor of four, the results match within statistical errors, suggesting the relation $\eta_d = 4\eta_m$. This relationship between η_m and η_d can be explained by the height model: the dimer value $d(\vec{r})$ at \vec{r} , is related to the product of neighboring spin operators, Eq. (7), which in the coarse-grained model can be considered simply as the square of the spin operator at \vec{r} , $(\sigma^z(\vec{r}))^2$. By representing the spin operators in terms of the height variables, one can relate the spin-spin and dimer-dimer correlation functions to the logarithmically diverging height difference profile; the observed factor of four relating η_d and η_m then emerges. For details, see the Supplemental Material, Sec. SII [12].

Scaling at $T = 0$. At the quantum critical point, there must be a different relationship between η_d and η_m . Given the irrelevance in 2 + 1 dimensions of \mathbb{Z}_4 or \mathbb{Z}_8 perturbations to a U(1) order parameter, the primary order parameter should scale with the conventional 3D XY critical exponent $1 + \eta_{3DXY}$ [29], as previously confirmed in simulations with a spin-based order parameter [10]. However, to explain the critical scaling of the dimer order parameter, we must reference other aspects of the field theory. Here we analyze both order parameters using simulations at $T = 1/L$.

We extract η_m from the asymptotic long distance ($r = L/2$) critical spin-spin correlation function, which is expected to scale as $C_M(L/2) \sim L^{-(1+\eta_m)} = L^{-2\Delta_\phi}$, where Δ_ϕ is the scaling dimension of the operator of the order parameter ϕ in the 3D O(2) theory. This is often referred to as a charge-1 (or spin-1) operator [17,30], indicating that it corresponds to a perturbation, e.g., $h \cos(\theta)$, inducing order in a single direction in the O(2) space, so that the degeneracy is completely lifted. A corresponding perturbation in FFTFIM would be one that fully breaks the \mathbb{Z}_8 symmetry in the ordered state, favoring one of the eight columnar spin configurations.

A perturbation that couples an external field to the secondary order parameter would not fully break the \mathbb{Z}_8 symmetry of the ground state, but would favor the two spin configurations of given columnar dimer state. Accordingly, in the low-energy U(1) theory the perturbation should be charge-2 (or spin-2 traceless symmetric) of the form $h \cos(2\theta)$, which can also be accomplished with products of ϕ components, e.g., $h\phi_1\phi_2$. This operator has scaling dimension often referred to as Δ_t [17,30],

To test the scaling form $L^{-(1+\eta_d)} = L^{-2\Delta_t}$, we analyze the oscillating part $C_D(L/2)$ of the dimer-dimer correlation function. Since the connection between the primary order parameter and Δ_ϕ is well known, we first used its scaling behavior to refine the value of Γ_c reported in Ref. [10], as detailed in the Supplemental Material, Sec. SV [12], obtaining $\Gamma_c = 1.57680 \pm 0.00009$. We then calculated $C_M(L/2)$ and $C_D(L/2)$ at the midpoint; their scaling behaviors are shown in Fig. 4. The results match very well the scaling dimensions obtained in recent numerical conformal bootstrap calculations [30]: $\Delta_\phi \approx 0.519088$ and $\Delta_t \approx 1.23629$.

The simplest effective model with the same microscopic symmetries and exhibiting the same scaling behavior is a classical 3D eight-state clock model, where a charge- l order parameter is defined by the vector $\vec{m}_l = (m_x, m_y)$, with $m_x = \sum_i \cos(l\theta_i)$, $m_y = \sum_i \sin(l\theta_i)$, θ_i being the angle of spin i . Results for this model are presented in Supplemental Material, Sec. SVI [12]). The excellent agreement with the expected

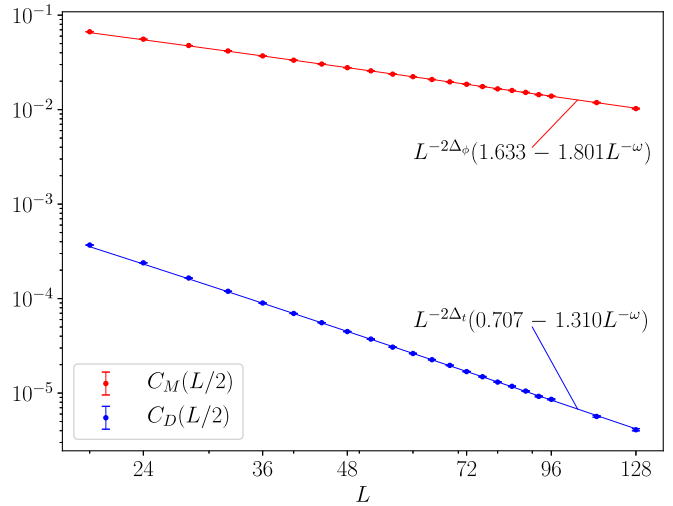


FIG. 4. Dimer-dimer (blue) and spin-spin (red) correlation functions at the quantum critical point, $\Gamma/J = 1.5768$. The lines are fits of the $L \geq 44$ data to the expected scaling form $\propto L^{-2\Delta_{s,t}}(a + bL^{-\omega})$, with $\Delta_\phi = 0.519088$, $\Delta_t = 1.23629$ [30], and the correction exponent $\omega = 0.789$ [31] in the 3D O(2) universality class. The reduced χ^2 values are ~ 0.8 and ~ 0.9 for the spin and dimer correlations, respectively.

exponents in both the FFTFIM and clock model confirms without doubt the emergent U(1) symmetry and the primary and secondary nature of the order parameters in the FFTFIM.

Conclusion. We have clarified the nature of the two order parameters, based on spins and dimers, in the square-lattice FFTFIM. The spin-based order parameter is primary, as it scales with the leading critical exponents and displays the full eightfold degeneracy of the ordered phase, while the \mathbb{Z}_4 dimer order parameter is secondary with faster decaying critical correlations. Our QMC results at $T = 0$ and $T > 0$ confirm the scaling exponents predicted from the respective low-energy field theories.

Mapping to dimer models is a powerful tool in the study of frustrated spin systems, and the problem of lattice coverings by hard-core dimers is an interesting topic in itself. The connection between the secondary dimer order parameter and the primary spin order parameter then provides a crucial link between the models that had not been previously drawn in this context. Beyond the particular FFTFIM considered here, the triangular and kagome lattice AF Ising models [23,32], the fully-frustrated honeycomb lattice Ising model [23], and the fully frustrated 4–8 lattice Ising models [33] are all well studied systems where the secondary order parameter prescription could also be applied.

Our insights also explain the critical scaling of a so-called “parasitic” order parameter studied in the AF three-state Potts model on the diamond lattice [1–3]. While this system primarily orders antiferromagnetically in the ground state, it was shown that the presence of this order induces a finite ferromagnetic moment, which is captured by a secondary order parameter. The observed scaling of this order parameter had previously eluded explanation, but it is now clear that this “parasitic” order parameter also has scaling dimension Δ_t in that system.

The relevance of the secondary order parameter operator ($\Delta_\tau < 3$) in the FFTFIM implies that a perturbation favoring one of the dimer states, accomplished by appropriately modulating the Ising couplings, will induce a \mathbb{Z}_2 symmetry breaking phase in the plane of Γ and the dimer field (modulation) strength h_d . The phase boundary between the paramagnetic and ordered phases should have the asymptotic form $h_{d,c} \sim |\Gamma_c(h_{d,c}) - \Gamma_c(0)|^{\nu/\nu_d}$, where ν is the 3D O(2) correlation-length exponent and $\nu_d = (3 - \Delta_\tau)^{-1}$, which we confirm in the Supplemental Material, Sec. SVII [12].

The FFTFIM, with $h_d = 0$ and $h_d > 0$, can be implemented on current D-Wave quantum annealing devices. While the frustrated AF triangular AF Ising model had already been

studied in depth [34,35], only recently was the FFTFIM implemented on such a device [36]. In this recent study, only the spin order parameter was investigated, and it would be interesting to study dimer order parameter as well, in the light of our results.

Acknowledgments. We would like to thank F. Alet, L. Wang, and S. Hearth for useful discussions. This work was supported by the Simons Foundation under Grant No. 511064, by the National Natural Science Foundation of China under Grants No. 12122502 and No. 12175015, and by the Swiss National Science Foundation under Grant No. 182179. Most of the numerical calculations were carried out on the Shared Computing Cluster managed by Boston University's Research Computing Services.

-
- [1] K. Hattori and H. Tsunetsugu, *J. Phys. Soc. Jpn.* **83**, 034709 (2014).
- [2] K. Hattori and H. Tsunetsugu, *J. Phys. Soc. Jpn.* **85**, 094001 (2016).
- [3] H. Tsunetsugu, T. Ishitobi, and K. Hattori, *J. Phys. Soc. Jpn.* **90**, 043701 (2021).
- [4] J. Villain, *J. Phys. C* **10**, 1717 (1977).
- [5] J. Villain, R. Bidaux, J.-P. Carton, and R. Conte, *J. Phys. France* **41**, 1263 (1980).
- [6] R. Moessner, *Can. J. Phys.* **79**, 1283 (2001).
- [7] C. L. Henley, *Phys. Rev. Lett.* **62**, 2056 (1989).
- [8] D. Blankschtein, M. Ma, and A. N. Berker, *Phys. Rev. B* **30**, 1362 (1984).
- [9] R. A. Jalabert and S. Sachdev, *Phys. Rev. B* **44**, 686 (1991).
- [10] S. Wenzel, T. Coletta, S. E. Korshunov, and F. Mila, *Phys. Rev. Lett.* **109**, 187202 (2012).
- [11] T. Coletta, S. E. Korshunov, and F. Mila, *Phys. Rev. B* **90**, 205109 (2014).
- [12] See Supplemental Material at <http://link.aps.org/supplemental/10.1103/PhysRevB.109.L140408> for the phase diagram, Binder-crossing finite-size scaling, height model mapping, analysis of correlation functions, determination of Γ_c , results for 3D classical clock model, and the \mathbb{Z}_2 phase boundary, which includes Refs. [37–44].
- [13] J. V. José, L. P. Kadanoff, S. Kirkpatrick, and D. R. Nelson, *Phys. Rev. B* **16**, 1217 (1977).
- [14] A. W. Sandvik, *Phys. Rev. E* **68**, 056701 (2003).
- [15] L. Wu, M. J. Young, Y. Shao, C. W. Garland, R. J. Birgeneau, and G. Heppke, *Phys. Rev. Lett.* **72**, 376 (1994).
- [16] A. Aharony, R. J. Birgeneau, C. W. Garland, Y.-J. Kim, V. V. Lebedev, R. R. Netz, and M. J. Young, *Phys. Rev. Lett.* **74**, 5064 (1995).
- [17] M. Hasenbusch and E. Vicari, *Phys. Rev. B* **84**, 125136 (2011).
- [18] R. R. Netz and A. Aharony, *Phys. Rev. E* **55**, 2267 (1997).
- [19] P. Calabrese and P. Parruccini, *Phys. Rev. B* **71**, 064416 (2005).
- [20] D. Blankschtein, M. Ma, A. N. Berker, G. S. Grest, and C. M. Soukoulis, *Phys. Rev. B* **29**, 5250 (1984).
- [21] H. W. J. Blöte and M. P. Nightingale, *Phys. Rev. B* **47**, 15046 (1993).
- [22] S. V. Isakov and R. Moessner, *Phys. Rev. B* **68**, 104409 (2003).
- [23] R. Moessner and S. L. Sondhi, *Phys. Rev. B* **63**, 224401 (2001).
- [24] J. Stephenson, *J. Math. Phys.* **11**, 413 (1970).
- [25] Y. Jiang and T. Emig, *Phys. Rev. Lett.* **94**, 110604 (2005).
- [26] S. E. Korshunov, *Phys. Rev. B* **86**, 014429 (2012).
- [27] C. L. Henley, *J. Stat. Phys.* **89**, 483 (1997).
- [28] B. Nienhuis, H. J. Hilhorst, and H. W. J. Blöte, *J. Phys. A: Math. Gen.* **17**, 3559 (1984).
- [29] M. Campostrini, M. Hasenbusch, A. Pelissetto, and E. Vicari, *Phys. Rev. B* **74**, 144506 (2006).
- [30] S. M. Chester, W. Landry, J. Liu, D. Poland, D. Simmons-Duffin, N. Su, and A. Vichi, *J. High Energy Phys.* **06** (2020) 142.
- [31] M. Hasenbusch, *Phys. Rev. B* **100**, 224517 (2019).
- [32] O. Nagai, S. Miyashita, and T. Horiguchi, *Phys. Rev. B* **47**, 202 (1993).
- [33] S. N. Hearth, S. C. Morampudi, and C. R. Laumann, *Phys. Rev. B* **105**, 195101 (2022).
- [34] A. D. King *et al.*, *Nature (London)* **560**, 456 (2018).
- [35] A. D. King *et al.*, *Nat. Commun.* **12**, 1113 (2021).
- [36] A. Ali, H. Xu, W. Bernoudy, A. Nocera, A. D. King, and A. Banerjee, [arXiv:2403.00091](https://arxiv.org/abs/2403.00091) [quant-ph].
- [37] K. Binder, *Phys. Rev. Lett.* **47**, 693 (1981).
- [38] Y.-D. Hsieh, Y.-J. Kao, and A. W. Sandvik, *J. Stat. Mech.: Theory Exp.* (2013) P09001.
- [39] M. E. Fisher, *Phys. Rev.* **124**, 1664 (1961).
- [40] D. S. Rokhsar and S. A. Kivelson, *Phys. Rev. Lett.* **61**, 2376 (1988).
- [41] F. Alet, J. L. Jacobsen, G. Misguich, V. Pasquier, F. Mila, and M. Troyer, *Phys. Rev. Lett.* **94**, 235702 (2005).
- [42] J. K. Burton, Jr., and C. L. Henley, *J. Phys. A* **30**, 8385 (1997).
- [43] H. Shao, W. Guo, and A. W. Sandvik, *Phys. Rev. Lett.* **124**, 080602 (2020).
- [44] Y. Jiang and T. Emig, *Phys. Rev. B* **73**, 104452 (2006).